ON THE LOCAL LINEAR INDEPENDENCE OF GENERALIZED SUBDIVISION FUNCTIONS

JÖRG PETERS AND XIAOBIN WU

Abstract. Characterizing the linear and local linear independence of the functions that span a linear space is a key task if the space is to be used computationally. Given the control net, the spanning functions of one spatial coordinate of a generalized subdivision surface are called nodal functions. They are the limit, under subdivision, of associating the value one with one node and zero with all others. No characterization of independence of nodal functions has not been published to date, even for the two most popular generalized subdivision algorithms, Catmull-Clark subdivision and Loop's subdivision. This paper provides a road map for the verification of linear and local linear independence of generalized subdivision functions. It proves the conjectured global independence of the nodal functions of both algorithms; disproves local linear independence (for higher valences); and establishes linear independence on every surface region corresponding to a facet of the control net. Subtle exceptions, even to global independence, underscore the need for a detailed analysis to provide a sound basis for a number of recently developed computational approaches.

Key words. Subdivision surfaces, Linear independence, Interpolation

1. Introduction. Subdivision algorithms create an ever tighter approximation of a smooth free-form surface by recursively refining and smoothing a polyhedral input mesh, known as control mesh (see Figure 1.1 below). The two most popular subdivision algorithms, Catmull-Clark and Loop, replace at each step one facet with four. Catmull-Clark meshes consist of four-sided facets [3] and Loop meshes consist of triangles [10]. The two refinement methods are very popular in graphics, and, although the resulting surfaces are not 'fair' enough for high-end industrial styling purposes [13], they are increasingly considered for computational purposes [8, 4]. It is therefore important to know whether the functions, associated with each control

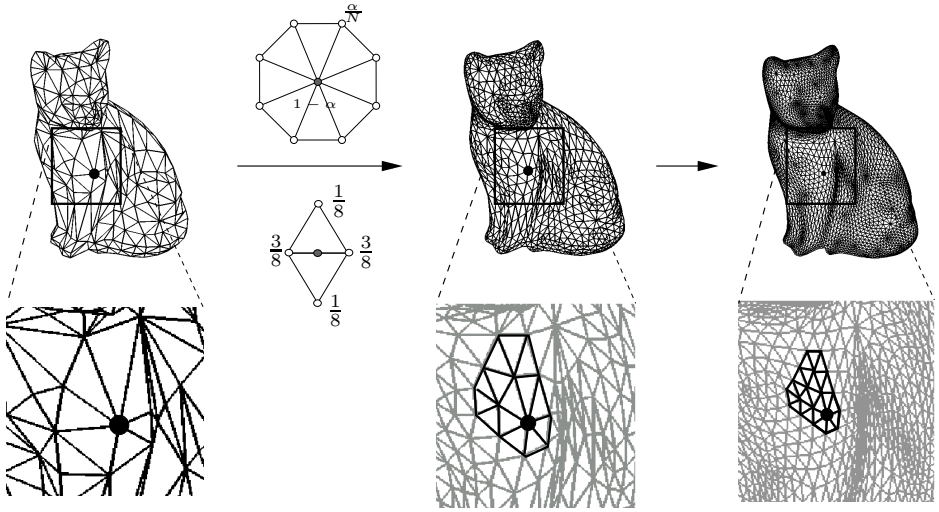

FIG. 1.1. *Modeling with Loop's subdivision. (top) A triangulated cat sculpture refined by Loop subdivision. Two stencils give the weights for averaging new nodes from old ones. The 'vertex rule' (above the arrow) is centrally symmetric with* $64\alpha := 40 - (3 + 2\cos(2\pi/N))^2$ *and preserves the number* N *of neighbors, i.e. the node's valence. The 'edge rule' creates nodes of valence six for each edge. (bottom, solid lines) Sequence of submeshes defining one of* $N = 7$ *triangular surface pieces that surround the limit point of the sequence of extraordinary nodes* $\bullet$.

node of the mesh, are linearly independent, or what dependence exists. Locally, on a fixed domain Ω, the pieces of the subdivision surfaces have the form $\sum_i \mathbf{a}_i \nu_i$, $\mathbf{a}_i \in \mathbb{R}^3$, i.e. they are a linear combination of *nodal functions* ν_i.

A number of publications have tacitly assumed that the nodal functions ν_i are linearly independent. Without proof, [8, 7, 4] call the nodal functions subdivision basis functions, [11] uses the nodal functions as scaling functions to form a 'basis' of the coarsest level of a multiresolution hierarchy, [12] fits subdivision surfaces by allowing one interpolation condition for each mesh node, and [16, 15, 18] call certain eigenfunctions (a set closely related to the set of nodal functions) an 'eigenbasis' and the analysis via universal surfaces [18] is error prone unless the nodal functions are independent. In fact, while generically true, for Catmull-Clark the assumption of linear independence of the nodal functions is false in some cases. The eight nodal functions of the simplest quadrilateral control mesh, a cube, are globally linearly dependent (see Lemma 4.1): in general, we cannot fit eight arbitrary data points by adjusting the coefficients $\mathbf{a}_i$ of the corresponding surface $\sum_{i=1}^{8} \mathbf{a}_i \nu_i$.

For the well-known tensor-product spline functions, (global) linear independence may be interpreted as linear independence over the checkerboard grid of the union of domain rectangles delineated by the knot lines and joined by identifying edges of the rectangles in the natural fashion. This definition generalizes to subdivision surfaces as follows. Let $\mathbf{\Omega}$ be a unit square if the kth facet of the control mesh has four vertices and a unit triangle if it has three vertices. Let Γ be the union of all domains $(\mathbf{\Omega}, k)$, indexed by their control mesh facet index, with edges topologically identified if the facets share edges. This gives Γ the structure of a 2-manifold homeomorphic to the control mesh. Global linear independence is linear independence with respect to Γ.

DEFINITION 1.1 (Global linear independence). *A set of nodal functions are* globally linearly independent *if they are independent over the domain manifold* Γ. *That is, if* $\forall \mathbf{u} \in \Gamma : \sum_i \mathbf{a}_i \nu_i(\mathbf{u}) = \mathbf{0}$ *then* $\mathbf{a}_i = 0$.

While some of the numerical methods require only standard (global) linear independence, others, such as local Hermite interpolation and localized multi-resolution, rely on stronger notions of independence. We need to analyze independence on certain ring-shaped annuli $\mathcal{A}$ and on subsets $\mathbf{\Omega}_i$ of the unit square or unit triangle $\mathbf{\Omega}$. The strongest and most subtle notion of independence is local linear independence.

DEFINITION 1.2 (Local linear independence). *A set of nodal functions are* locally linearly independent *if for any bounded open* $G \subseteq \Gamma$*, all the nodal functions having some support in* G *are linearly independent on* G.

Remarkably, for box-splines and B–splines, the standard notion of (global) linear independence is equivalent to local linear independence [5], (II.57)Theorem p. 51. That is, if all coefficients $\mathbf{a}_i$ have to vanish in order that $\sum_i \mathbf{a}_i \nu_i \equiv \mathbf{0}$, (global linear independence), then the coefficients of all nodal functions that are nonzero on any open set G have to vanish if $\sum_i \mathbf{a}_i \nu_i$ vanishes on G (local linear independence). Since G can be arbitrarily small, local linear independence is a stricter requirement on the nodal functions than global linear independence. By contrast, local and global independence are not equivalent for subdivision nodal functions. This observation provides rare insight into the structural difference between subdivision and spline surfaces. Specifically, we show that for Catmull-Clark and Loop subdivision

(i) the nodal functions are globally linearly independent[1];

[1] with one exception: Catmull-Clark applied to nodes with valence $N = 3$; see Lemma 4.1

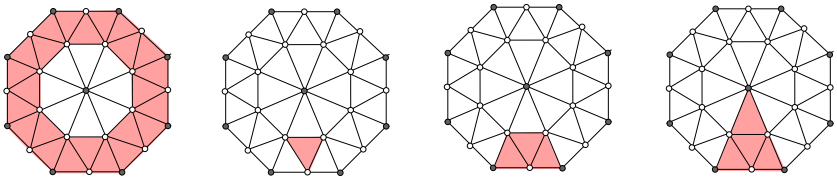

$\forall N$ (Lemma 2.2) | $N \leq 6$ (Lemma 3.2) | $N \leq 7$ (Conjecture 1) | $\forall N$ (Theorem 3.6)

FIG. 1.2. *Summary of findings for Loop subdivision. Domains G (shaded) and valence N for which the nodal functions with support on G are linearly independent.*

(ii) the nodal functions are linearly independent over an annulus[1] such as in Figure 1.2, *left*;

(iii) for valence N higher than the 'regular' valence, the nodal functions are not locally linearly independent;

(iv) the nodal functions are linearly independent on each domain $\mathbf{\Omega}$ naturally associated with one facet of the control net[1].

Points (i)–(iv) have direct implications on interpolation (to be compared with the Schoenberg-Whitney theorem of spline interpolation). Consider interpolation with Loop subdivision surfaces. If all three vertices of a facet have valence six, interpolating 12 data points on a domain $\mathbf{\Omega}$ is a well-posed problem with a unique solution. However, if one of the vertices has valence $N < 6$ then matching 12 data represents too many contraints; if it has $N > 6$ then the fitting problem is underconstrained. If we choose the number of interpolation conditions to equal the number of nodal functions that are nonzero on $\mathbf{\Omega}$, i.e. if we specify $N+6$ interpolation points, we find that, if the points belong to a subregion $\mathbf{\Omega}_1$ the problem is overconstrained for $N > 6$. ($\mathbf{\Omega}_1$ is the shaded area in Figure 1.2, labelled Conjecture 1.) Interpolation with Catmull-Clark subdivision follows a similar pattern with an additional complication for $N = 3$.

The analysis is made easier by the fact that the component functions of most popular subdivision schemes, and in particular of both Catmull-Clark and Loop subdivision, are variations of the well-understood box-spline subdivision [5]; much of the subdivision limit surfaces, corresponding to quads with 4-valent vertices, respectively triangles with 6-valent vertices are 'regular', i.e. are spline surfaces generated by box-splines. This box-spline connection should make us cautious since the shifts of box-splines are, in general, not linearly independent. For example, the four-direction (quincunx) subdivision, which gives rise to 4-8 subdivision [17], has dependent nodal functions. Catmull-Clark subdivision rules generalize the two-direction box-spline rules, i.e. the rules of the bicubic tensor-product spline; and Loop subdivision generalizes a three-direction box-spline, the convolution of the linear 'hat' function with itself. For both splines we know [5] that the nodal functions form a basis and therefore are independent. This means, we can focus on submeshes that define the neighborhood of extraordinary nodes, where the connectivity of the control mesh differs from the regular connectivity of the box spline, namely submeshes surrounding nodes of valence $N \neq 4$ for Catmull-Clark meshes and of valence $N \neq 6$ for Loop meshes. We do not assume that all direct neighbors of these extraordinary nodes are of regular valence.

We first discuss Loop's subdivision, proposed for computational purposes in [8, 7, 4], then Catmull-Clark subdivision, then generalize the key results.

2. Loop Subdivision. A subdivision algorithm states how a new node is computed from a (small local) submesh of old nodes, and how this new node is to be connected to other new nodes. In particular, for Loop subdivision, there are only two rules: to compute new nodes, corresponding to edges of the old mesh, and to compute new nodes, corresponding to old nodes. These rules are expressed by the two stencils (weighted neighborhood graphs) in Figure 1.1, above and below the arrow. A node of a Loop mesh is *extraordinary* if it does not have six neighbors.

Due to the small footprint of the rules, a submesh consisting of one triangle and all triangles attached to it defines, by going to the limit, a triangular piece of the surface adjacent to the limit of the extraordinary node. If all nodes of the central triangle are of valence six, the surface is a polynomial piece of a three-direction box spline and its properties are well understood. Since new edge nodes have valence six, extraordinary nodes are more and more isolated under refinement, and we can focus on triangles with one extraordinary node of valence $N \neq 6$. In the following, the subscript 0 refers to a mesh where any two extraordinary nodes are separated by at least one node of valence six. This may be the result of one subdivision applied to the original mesh.

While the typical application of Loop subdivision creates a parametrized surface in $\mathbb{R}^3$, *for the analysis it is sufficient to look at one spatial coordinate since the coordinates do not interact.* The nodal function ν_i may then be defined by choosing an association of the control points a_j with the domain, setting one scalar control point a_i to 1 and all others to 0 and applying subdivision. The relevant submesh defining the triangular surface piece consists of $K := N + 6$ nodes that can be labeled as in Figure 2.1 (*top, left*). We store the submesh as a vector

$$\mathbf{c}_0 := (\mathbf{c}_{0,1}, \dots \mathbf{c}_{0,K}) \in \mathbb{R}^K.$$

Subdivision generates a new set of $M := K+6$ control vertices as shown in Figure 2.1 (top, right). We store those control vertices in a new vector

$$\mathbf{c}_1 := (\mathbf{c}_{1,1}, \dots, \mathbf{c}_{1,K}, \mathbf{c}_{1,K+1}, \dots \mathbf{c}_{1,M}).$$

If we represent the averaging rules as rows of a $M \times K$ matrix $\mathbf{A}$ (with row sum one), then the subdivision rules to compute the vector $\mathbf{c}_1$ from $\mathbf{c}_0$ are

$$\mathbf{c}_1 = \mathbf{A}\mathbf{c}_0 \text{ where } \mathbf{A} := \begin{pmatrix} \mathbf{A}_{11} & 0 \\ \mathbf{A}_{21} & \mathbf{A}_{22} \\ \mathbf{A}_{31} & \mathbf{A}_{32} \end{pmatrix}.$$

Here $\mathbf{A}_{11}$ is an $(N+1) \times (N+1)$ matrix that computes the new extraordinary node and the vertices adjacent to it (note that this also holds for an optional initial refinement to generate $\mathbf{c}_0$ from a mesh that has neighboring extraordinary nodes); $\mathbf{A}_{21}$ and $\mathbf{A}_{22}$ determine the five vertices with indices $N+4, N+3, N+2, N+5, N+6$ of the next layer; and $\mathbf{A}_{31}$ and $\mathbf{A}_{32}$ define the six outermost nodes. The sizes of $\mathbf{A}_{22}$ and $\mathbf{A}_{32}$ are 5×5 and 6×5 respectively. Leaving out the direct neighbors of the extraordinary node, $\mathbf{c}_{1,4}, \mathbf{c}_{1,5}, \dots, \mathbf{c}_{1,N-1}$, the remaining control points

$$\mathbf{c}_1^{\text{box}} := (\mathbf{c}_{1,1}, \mathbf{c}_{1,2}, \mathbf{c}_{1,3}, \mathbf{c}_{1,N}, \dots \mathbf{c}_{1,M})$$

define three triangular polynomial pieces shown as shaded in Figure 2.1 (top,right).

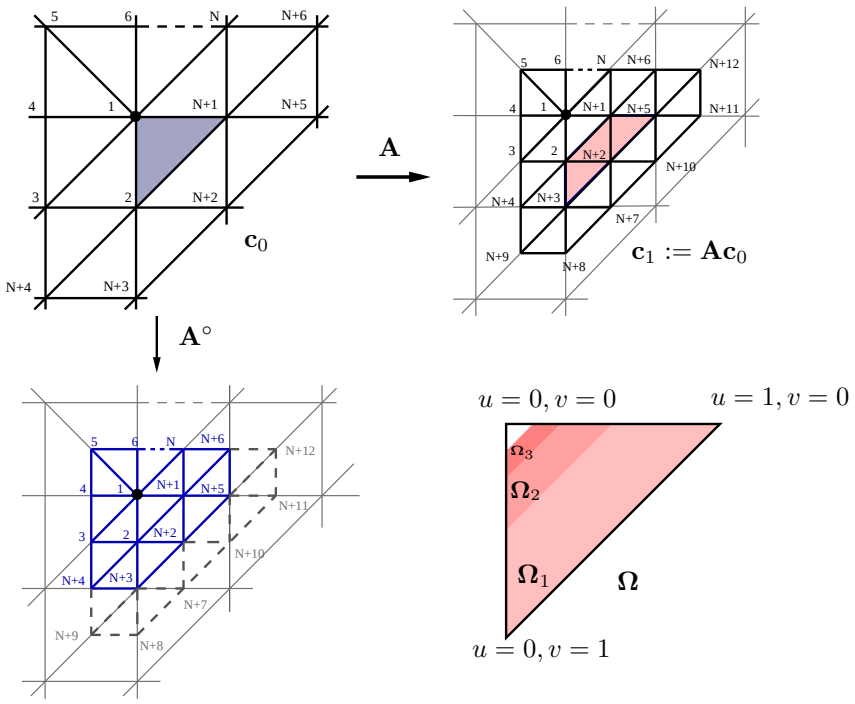

FIG. 2.1. *(top,left) Labeling of the submesh that defines a triangular surface piece (schematically represented by the shaded area) near an extraordinary node (label 1). (top,right) Refined submesh,* $\mathbf{A}\mathbf{c}_0$*. (bottom,left) Refined submesh,* $\mathbf{A}^\circ\mathbf{c}_0$*, used to evaluate the next spline ring. (bottom,right) The domain* $\mathbf{\Omega}$ *of the composite triangular surface piece consists of an infinite sequence of quadrilateral (chopped triangle) subdomains. The first three such subdomains,* $\mathbf{\Omega}_1$*,* $\mathbf{\Omega}_2$*,* $\mathbf{\Omega}_3$*, are shaded.*

To compute the nodes of the next subdivision step, we need only the first K control points of $\mathbf{c}_1$ (see Figure 2.1 bottom left),

$$(\mathbf{c}_{1,1}, \mathbf{c}_{1,2}, \ldots, \mathbf{c}_{1,K}) = \mathbf{A}^\circ\mathbf{c}_0 := \begin{pmatrix} \mathbf{A}_{11} & 0 \\ \mathbf{A}_{21} & \mathbf{A}_{22} \end{pmatrix} \mathbf{c}_0.$$

By repeating the process, an infinite sequence of piecewise polynomial rings is generated. We can choose their domains $\mathbf{\Omega}_\ell$ so that their union fills out the triangular domain $\mathbf{\Omega}$:

$$\mathbf{\Omega} := \{(u,v) | u+v+w = 1, u, v, w \geq 0\} = \cup_{\ell=1}^{\infty} \mathbf{\Omega}_\ell \qquad \mathbf{\Omega}_1 := \mathbf{\Omega} \backslash \frac{1}{2}\mathbf{\Omega}, \quad \mathbf{\Omega}_{\ell+1} := \frac{1}{2}\mathbf{\Omega}_\ell.$$

The control vertices $\mathbf{c}_n$ after n subdivision steps that determine the function on $\mathbf{\Omega}_n$ are:

$$\mathbf{c}_n = \mathbf{A}(\mathbf{A}^\circ)^{n-1}\mathbf{c}_0, \qquad n \geq 1. \tag{2.1}$$

From the recursion in Equation 2.1, it is evident that the eigenstructure of $\mathbf{A}^\circ$ plays a crucial rule in determining the properties of the subdivision surfaces such as the computation of the limit position, tangent plane, and shape analysis [6, 1, 14, 13, 9].

Using Fourier transform, it is easy to derive the vector of eigenvalues $\mathbf{\Lambda}_{11}$ of $\mathbf{A}_{11}$,

$$\mathbf{\Lambda}_{11} := [1, \frac{5}{8} - \alpha(N), f(1), \ldots, f(N-1)]$$

where

$$f(k) := \frac{3 + 2\cos(2\pi k/N)}{8}, \qquad \alpha(N) := \frac{5}{8} - f(1)f(1),$$

and $\mathbf{\Lambda}_{22}$ of $\mathbf{A}_{22}$:

$$\mathbf{\Lambda}_{22} := [\frac{1}{8}, \frac{1}{8}, \frac{1}{8}, \frac{1}{16}, \frac{1}{16}].$$

Except for the case $N = 3$, $\mathbf{A}^\circ$ can be diagonalized by the matrix $\mathbf{V}$ of its eigenvectors (details of the eigenanalysis of $\mathbf{A}^\circ$ can be found e.g. in [15]):

$$\mathbf{A}^\circ = \mathbf{V}\mathbf{\Lambda}\mathbf{V}^{-1}, \quad \mathbf{\Lambda} = \mathrm{diag}(\mathbf{\Lambda}_{11}, \mathbf{\Lambda}_{22}), \mathbf{V} = \begin{pmatrix} \mathbf{U}_0 & 0 \\ \mathbf{U}_1 & \mathbf{W}_1 \end{pmatrix} \tag{2.2}$$

where the submatrices $\mathbf{U}_0$ and $\mathbf{W}_1$ are the eigenvectors of $\mathbf{A}_{11}$ and $\mathbf{A}_{22}$, respectively. For $N > 3$, the columns of $\mathbf{V}$ are linearly independent vectors in $\mathbb{R}^K$.

Now let the initial submesh $\mathbf{c}_0 := \mathbf{v}_i$ be an eigenvector associated with eigenvalue λ_i and φ_i the corresponding linear combination of nodal functions. Then, after n steps of subdivision,

$$\mathbf{c}_n|_{\mathbf{c}_0=\mathbf{v}_i} = \mathbf{A}(\mathbf{A}^\circ)^{n-1}\mathbf{v}_i = \mathbf{A}\lambda_i^{n-1}\mathbf{v}_i = \lambda_i^{n-1}\mathbf{A}\mathbf{v}_i = \lambda_i^{n-1}\mathbf{c}_1|_{\mathbf{c}_0=\mathbf{v}_i}.$$

Therefore $\varphi_i(\mathbf{\Omega}_{n+1})$ is a scaled multiple of $\varphi_i(\mathbf{\Omega}_1)$. Precisely,

$$\forall (u, v) \in \mathbf{\Omega} \text{ and } \forall n \geq 1, \varphi_i(\frac{u}{2^n}, \frac{v}{2^n}) = \lambda_i^n \varphi_i(u, v). \tag{2.3}$$

In [15] these K functions φ_i are called eigenbasis. However, adjacent to an extraordinary node, each φ_i consists of an infinite union of polynomial pieces. The subtle but important point to be settled here is that, even if the columns of $\mathbf{V}$ are independent, the corresponding functions can be dependent. We therefore call the functions φ_i *eigenfunctions*. We note that, to be scalable, the control net of an eigenfunction are only well-defined if the extraordinary node is surrounded by regular nodes. For the proofs of independence of *nodal functions*, we will be allowed to assume that the extraordinary node is isolated. An *extraordinary node is isolated* if it is surrounded by regular nodes. For, if $\mathbf{c}_0$ is isolated as the result of one refinement, and we show that $\mathbf{c}_0$ is zero then also the values associated with the unrefined nodes must be zero since the matrix $\mathbf{A}_{11}$ that maps the original nodes to the refined nodes is of full rank for all valences. To see that $\mathbf{A}_{11}$ is of full rank also for $N = 3$, we need only observe that $\Lambda_{11} = [1, f(1)f(1), f(1), f(1)]$, $f(1) = 1/4$ and the eigenvectors of $f(1)$ are independent.

LEMMA 2.1. $\mathbf{A}_{11}$ *is of full rank for all valences.*

To show that subdivision near extraordinary nodes is similar to but different from spline representations, we will show that the eigenfunctions are linearly independent over $\mathbf{\Omega}$, but linearly dependent on certain subsets of $\mathbf{\Omega}$.

To show that the nodal functions of Loop subdivision are (globally) linearly independent, we focus on subdomains that form an annulus surrounding the preimage of a sequence of extraordinary nodes. With the natural topological identification of edges to induce the structure of a 2-manifold with two boundaries, we define an annulus as N copies of $\mathbf{\Omega}_1$,

$$\mathcal{A} := \{1, \ldots, N\} \times \mathbf{\Omega}_1.$$

Note that this requires that the extraordinary node is isolated.

LEMMA 2.2. *The nodal functions of Loop subdivision with support on $\mathcal{A}$ are linearly independent over $\mathcal{A}$.*

Proof. For $\mathcal{A}$ to be well-defined, the extraordinary node must be isolated. Let $f := \sum_i \mathbf{c}_{0,i}\nu_i$ is zero on all of $\mathcal{A}$. Then the subset of nodes $\mathbf{c}_1^{\text{box}}$ can be interpreted as a regular three-direction box-spline control net defining three polynomial pieces near the extraordinary node. Since the box-splines are locally linearly independent [5], all box-spline control points defining f on $\mathcal{A}$ are zero. Since all eigenvalues of $\mathbf{A}^\circ$ are positive for $N > 3$, $\mathbf{A}^\circ$ is of full rank and for $N = 3$, Lemma 3.5 shows that the matrix M is of full rank. Therefore all $\mathbf{c}_{0,i}$ must be zero. □

Now consider *all* nodal functions of a once-refined control net. Lemma 2.2 proves linear independence of these nodal functions on the union of all annuli $\mathcal{A}$. By Lemma 2.1, also the original control nodes must be zero if the function vanishes on all annuli.

COROLLARY 2.3. *The nodal functions of Loop subdivision are globally linearly independent.*

3. Local linear independence of Loop subdivision. In this section, we characterize the local linear independence of Loop subdivision nodal functions.

LEMMA 3.1. *For general N, the nodal functions of Loop subdivision are* not locally linearly independent. *Specifically, for any k there exists a valence N so that the nodal functions of Loop subdivision with support on $\mathbf{\Omega}_k$, $\nu_i, i = 1 \dots N+6$, are* locally linearly dependent *on $\mathbf{\Omega}_k$ and even on $\cup_{\ell=1}^k \mathbf{\Omega}_\ell$.*

Proof. All nodal functions corresponding to $\mathbf{c}_0$ have support (are nonzero) on each subdomain $\mathbf{\Omega}_k$. Each vector $\mathbf{c}_k^{\text{box}}$ corresponding to $\mathbf{\Omega}_k$ has 16 entries. For sufficiently large valence, the nodal functions on $\mathbf{\Omega}_k$ must therefore be dependent. By the same reasoning, for sufficiently large valence, the nodal functions on $\cup_{\ell=1}^k \mathbf{\Omega}_\ell$, for finite k, must be dependent. □

As could be hoped by the failure of the above counting argument, nodal functions are locally linearly independent for sufficiently low valence N.

LEMMA 3.2. *For $N \leq 6$ the nodal functions $\nu_i, i = 1 \dots N+6$, are locally linearly independent.*

Proof. Denote by $\mathbf{P}_i, i = 1, 2, 3$ the three $12 \times (N + 12)$ picking matrices that select the box-spline coefficients of each of the three triangular domain parts. Since $\mathbf{P}_i\mathbf{A}, i = 1, 2, 3$ is of full rank $\mathbf{c}_0$ must be zero if the 12 box-spline control points are zero. Then local linear independence of the three-direction box spline implies the claim on $\mathbf{\Omega}_1$. Since the control points on $\mathbf{\Omega}_\ell$ are computed from $\mathbf{c}_0$ by applying

$$\mathbf{P}_i\mathbf{A}(\mathbf{A}^\circ)^{\ell-1}$$

local linear independence on $\mathbf{\Omega}_1$ implies local linear independence on $\mathbf{\Omega}_\ell$ for $N > 3$. For $N = 3$, the claim follows from Lemma 3.5. □

For $N = 7$, the nodal functions are independent on $\mathbf{\Omega}_1$ and hence on $\cup_{\ell=1}^k \mathbf{\Omega}_\ell$, but, due to the dimension of the three polynomial pieces corresponding to $\mathbf{\Omega}_1$, they are not linearly independent on subsets of $\mathbf{\Omega}_1$ that do not straddle all three piecewise polynomial domains. As the valence N increases, a subtle pattern emerges.

CONJECTURE 1. *For $k := \lfloor (N-6)/2 \rfloor + 1 > 1$, the nodal functions of Loop subdivision $\nu_i, i = 1 \dots N+6$ are linearly independent on $\cup_{i=1}^{k} \mathbf{\Omega}_i$ and linearly dependent on $\cup_{i=1}^{k-1} \mathbf{\Omega}_i$.*

We verified the conjecture for isolated extraordinary nodes by symbolic calculation up to $N = 30$ which should cover most cases of practical interest.

To investigate linear independence on the natural domains corresponding to control facets, namely on $\mathbf{\Omega} = \cup_{\ell=1}^{\infty} \mathbf{\Omega}_\ell$, we need a better strategy. We use the eigenproperty of the eigenfunctions, that additional layers are scaled copies of the earlier layers.

LEMMA 3.3. *For valence $N > 3$, the* eigenfunctions φ_i, $i = 1, \dots N+6$, *of Loop subdivision are linearly independent on $\mathbf{\Omega}$.*

Proof. The proof is by contradiction. All eigenvalues λ_i of $\mathbf{A}^\circ$ are positive. We sort the eigenfunctions φ_i $(i = 1, \dots N+6)$ so that their associated eigenvalues λ_i descend from the largest to the smallest. Suppose there exist scalars $a_1, a_2, \dots a_{N+6}$, not all zero, such that

$$\sum_{i=1}^{N+6} a_i \varphi_i = 0.$$

Let λ_j be the largest eigenvalue such that $a_j \neq 0$. Then with $w_i := -a_i/a_j$, we write

$$\varphi_j = \sum_{i=j+1}^{N+6} w_i \varphi_i.$$

For $\forall (u,v) \in \mathbf{\Omega}$ and $\forall n \geq 1$, $(\frac{u}{2^n}, \frac{v}{2^n}) \in \mathbf{\Omega}$, with the above equation and equation (2.3), we have

$$\begin{aligned} \varphi_j(\frac{u}{2^n}, \frac{v}{2^n}) &= \sum_{i=j+1}^{N+6} w_i \varphi_i(\frac{u}{2^n}, \frac{v}{2^n}) \\ \Rightarrow \lambda_j^n \varphi_j(u,v) &= \sum_{i=j+1}^{N+6} w_i \lambda_i^n \varphi_i(u,v) \\ \Rightarrow \varphi_j(u,v) &= \sum_{i=j+1}^{N+6} w_i (\frac{\lambda_i}{\lambda_j})^n \varphi_i(u,v) \end{aligned}$$

Since $(\frac{\lambda_i}{\lambda_j})^n \to 0$ as $n \to \infty$ unless $\lambda_i = \lambda_j$,

$$\varphi_j(u,v) = \sum_{i \in \{i | \lambda_i = \lambda_j\}} w_i \varphi_i(u,v).$$

must hold. Therefore the eigenfunctions associated with λ_j must be linearly dependent. In the remainder of the proof, we show this to be false. In other words, the problem of proving the linear independence of all eigenfunctions has been reduced to the independence of the eigenfunctions with the same eigenvalue.

Because of the eigenstructure of $\mathbf{A}^\circ$, the multiplicities of its eigenvalues are small (at most four) and do not increase with N. Recall that the eigenvalues of $\mathbf{A}^\circ$ are

$$[1, \frac{5}{8} - \alpha(N), f(1), \dots, f(N-1), \frac{1}{8}, \frac{1}{8}, \frac{1}{8}, \frac{1}{16}, \frac{1}{16}].$$

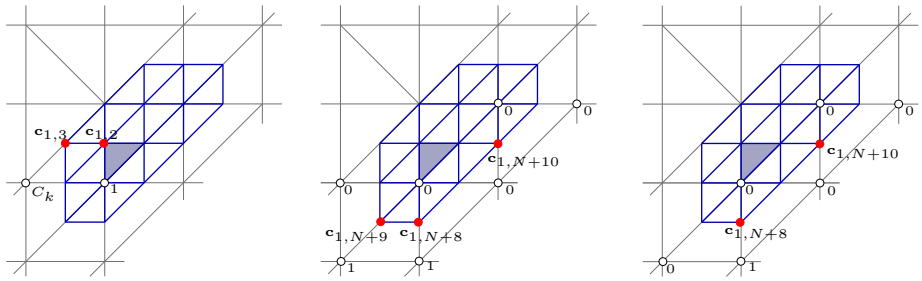

FIG. 3.1. *The box-spline control points* $\mathbf{c}_{1,i}$ *(solid dots) used to certify that pairs and triples of eigenfunctions are independent.*

where

$$\alpha(N) := \frac{5}{8} - \frac{(3+2\cos(2\pi/N))^2}{64}, f(k) := \frac{3+2\cos(2\pi k/N)}{8}.$$

To find the repeated eigenvalues, we observe that for $k \in \{1 \dots N-1\}$,

1. $f(k) = f(N-k)$,
2. if N is even and $k = N/2$, $f(k) = \frac{1}{8}$; otherwise $f(k) \notin \{\frac{1}{8}, \frac{1}{16}\}$.
3. $f(k) \neq 1$ and $f(k) \neq \frac{5}{8} - \alpha(N)$,

That is, if λ is an eigenvalue of $\mathbf{A}$ with multiplicity greater than one then $\lambda = f(k) \neq \frac{1}{8}$, or $\lambda = \frac{1}{8}$, or $\lambda = \frac{1}{16}$. In particular, all relevant eigenvalues are nonzero. We look at each case individually.

- Case 1: $\lambda = f(k) \neq \frac{1}{8}$
  In this case λ has multiplicity 2 and the associated eigenvectors $\mathbf{u}_k$ and $\mathbf{w}_k$ are given in [15]:

$$\mathbf{u}_k^T = (0, 1, C_k, C_{2k}, \dots C_{(N-1)k}, \dots) \qquad \text{and}$$
$$\mathbf{w}_k^T = (0, 0, S_k, S_{2k}, \dots S_{(N-1)k}, \dots)$$

  where $C_k := \cos(2\pi k/N)$ and $S_k := \sin(2\pi k/N)$. To show the two eigenfunctions defined by $\mathbf{u}_k$ and $\mathbf{w}_k$ are linearly independent, we consider the two box-spline entries of $\mathbf{c}_{1,2}$ and $\mathbf{c}_{1,3}$ (solid dots in Figure 3.1, *left*) after one step of subdivision applied to the mesh $\mathbf{c}_0 := \mathbf{u}_k$ and one step applied with $\mathbf{c}_0 := \mathbf{w}_k$. The two corresponding eigenfunctions are independent because

$$\det \begin{pmatrix} \mathbf{c}_{1,2}|_{\mathbf{c}_0=\mathbf{u}_k} & \mathbf{c}_{1,3}|_{\mathbf{c}_0=\mathbf{u}_k} \\ \mathbf{c}_{1,2}|_{\mathbf{c}_0=\mathbf{w}_k} & \mathbf{c}_{1,3}|_{\mathbf{c}_0=\mathbf{w}_k} \end{pmatrix} = \lambda^2 \det \begin{pmatrix} 1 & C_k \\ 0 & S_k \end{pmatrix} \neq 0,$$

  since $S(k) \neq 0$ because $f(k) \neq \frac{1}{8}$ and hence $k \neq \frac{N}{2}$.
- Case 2: $\lambda = \frac{1}{8}$
  In this case λ can have multiplicity of 3 or 4. We first show that the eigenfunctions corresponding to first three columns $\mathbf{y}_1, \mathbf{y}_2, \mathbf{y}_3$ of $\begin{pmatrix} 0 \\ \mathbf{W}_1 \end{pmatrix}$ are independent. The eigendecomposition (2.2) of $\mathbf{A}_{22}$ is (see [15]):

$$\mathbf{W}_1 = \begin{pmatrix} 0 & 0 & 1 & 0 & 0 \\ 1 & 0 & 1 & 0 & 1 \\ 1 & 0 & 0 & 0 & 0 \\ 0 & 1 & 1 & 1 & 0 \\ 0 & 1 & 0 & 0 & 0 \end{pmatrix}.$$

The independence of the eigenfunctions follows from the independence of the three box spline control points $\mathbf{c}_{1,N+8}, \mathbf{c}_{1,N+9}, \mathbf{c}_{1,N+10}$ (solid dots in Figure 3.1 *middle*) after one subdivision :

$$\det \begin{pmatrix} \mathbf{c}_{1,N+8}|_{\mathbf{c}_0=\mathbf{y}_1} & \mathbf{c}_{1,N+9}|_{\mathbf{c}_0=\mathbf{y}_1} & \mathbf{c}_{1,N+10}|_{\mathbf{c}_0=\mathbf{y}_1} \\ \mathbf{c}_{1,N+8}|_{\mathbf{c}_0=\mathbf{y}_2} & \mathbf{c}_{1,N+9}|_{\mathbf{c}_0=\mathbf{y}_2} & \mathbf{c}_{1,N+10}|_{\mathbf{c}_0=\mathbf{y}_2} \\ \mathbf{c}_{1,N+8}|_{\mathbf{c}_0=\mathbf{y}_3} & \mathbf{c}_{1,N+9}|_{\mathbf{c}_0=\mathbf{y}_3} & \mathbf{c}_{1,N+10}|_{\mathbf{c}_0=\mathbf{y}_3} \end{pmatrix} = \frac{1}{8^3} \det \begin{pmatrix} 4 & 4 & 0 \\ 0 & 0 & 1 \\ 1 & 4 & 4 \end{pmatrix} \neq 0.$$

If the multiplicity of $\frac{1}{8}$ is three, then we are done. Otherwise, $\lambda = f(N/2)$ for N even and we have one additional eigenvector $\mathbf{u}_k$ from $\begin{pmatrix} \mathbf{U}_0 \\ \mathbf{U}_1 \end{pmatrix}$. After one subdivision, the box-spline control point $\mathbf{c}_{1,3}$ is zero for $\mathbf{y}_1, \mathbf{y}_2, \mathbf{y}_3$ and nonzero for $\mathbf{u}_k$. This proves independence of all four eigenfunctions.

- Case 3: $\lambda = \frac{1}{16}$
  The eigenvectors of the two eigenfunctions associated with $\frac{1}{16}$ correspond to the last two columns $\mathbf{z}_1$ and $\mathbf{z}_2$ of $\begin{pmatrix} 0 \\ \mathbf{W}_1 \end{pmatrix}$. Pairwise independence follows from the independence of the two box spline control points $\mathbf{c}_{1,N+8}, \mathbf{c}_{1,N+10}$ (solid dots in Figure 3.1 *right*)

$$\det \begin{pmatrix} \mathbf{c}_{1,N+8}|_{\mathbf{c}_0=\mathbf{z}_1} & \mathbf{c}_{1,N+10}|_{\mathbf{c}_0=\mathbf{z}_1} \\ \mathbf{c}_{1,N+8}|_{\mathbf{c}_0=\mathbf{z}_2} & \mathbf{c}_{1,N+10}|_{\mathbf{c}_0=\mathbf{z}_2} \end{pmatrix} = \frac{1}{8^2} \det \begin{pmatrix} 0 & 3 \\ 3 & 0 \end{pmatrix} \neq 0.$$

This completes the proof of Lemma 3.3. □

We can now address our original goal of showing that the nodal functions ν_i are linearly independent.

COROLLARY 3.4. *For $N > 3$, the nodal functions of Loop subdivision, $\nu_i, i = 1 \ldots N+6$, are linearly independent on $\mathbf{\Omega}$.*

Proof. Each nodal function ν_i is generated by subdivision when setting control point i to 1 and all others to 0. If the extraordinary node is surrounded by regular nodes,

$$[\varphi_1, \ldots, \varphi_K] = \mathbf{V}[\nu_1, \ldots, \nu_K], \qquad K = N+6,$$

and independence follows since, for $N > 3$, the matrix $\mathbf{V}$ of eigenvectors is an invertible matrix. The general case follows by one step of subdivision and the full rank of $\mathbf{A}_{11}$. □

For the special case $N = 3$, the matrix $\mathbf{A}^\circ$ has a non-trivial Jordan block and can not be diagonalized. However, since the number of the nodal functions is small, namely nine, we need not decompose into the eigenspace.

LEMMA 3.5. *For $N = 3$, the nodal functions of Loop subdivision, $\nu_i, i = 1 \ldots N+6$, are linearly independent on $\mathbf{\Omega}$.*

Proof. If the extraordinary node is isolated, we explicitly determine the $(N+12) \times 9$ matrix $\mathbf{M}$ that maps $\mathbf{c}_0$ to the box-spline control points $\mathbf{c}_1^{\text{box}}$.

$$\frac{1}{16} \begin{bmatrix} 7 & 3 & 3 & 3 & 0 & 0 & 0 & 0 & 0 \\ 6 & 6 & 2 & 2 & 0 & 0 & 0 & 0 & 0 \\ 6 & 2 & 6 & 2 & 0 & 0 & 0 & 0 & 0 \\ 6 & 2 & 2 & 6 & 0 & 0 & 0 & 0 & 0 \\ 2 & 6 & 0 & 6 & 2 & 0 & 0 & 0 & 0 \\ 1 & 10 & 1 & 1 & 1 & 1 & 1 & 0 & 0 \\ 2 & 6 & 6 & 0 & 0 & 0 & 2 & 0 & 0 \\ 1 & 1 & 1 & 10 & 1 & 0 & 0 & 1 & 1 \\ 2 & 0 & 6 & 6 & 0 & 0 & 0 & 0 & 2 \\ 0 & 6 & 0 & 2 & 6 & 2 & 0 & 0 & 0 \\ 0 & 6 & 0 & 0 & 2 & 6 & 2 & 0 & 0 \\ 0 & 6 & 2 & 0 & 0 & 2 & 6 & 0 & 0 \\ 0 & 2 & 0 & 6 & 6 & 0 & 0 & 2 & 0 \\ 0 & 0 & 0 & 6 & 2 & 0 & 0 & 6 & 2 \\ 0 & 0 & 2 & 6 & 0 & 0 & 0 & 2 & 6 \end{bmatrix}.$$

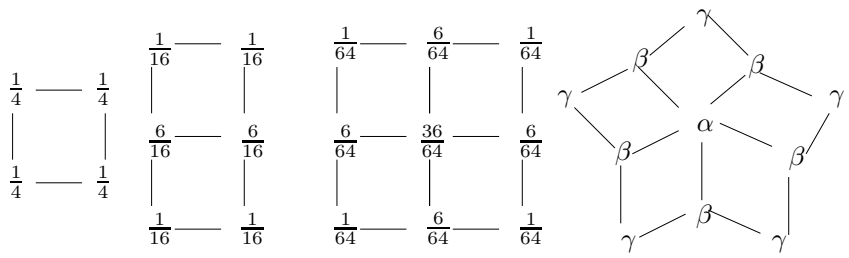

FIG. 4.1. *Refinement stencils of generalized Catmull-Clark subdivision.*

Since $\mathbf{M}$ has full rank and since the box-splines associated with each of $\mathbf{c}_{1,1}, \mathbf{c}_{1,2} \dots \mathbf{c}_{1,N+12}$ are linearly independent, the $\nu_i, i = 1 \dots 9$ are also linearly independent. The general case follows by one step of subdivision and the full rank of $\mathbf{A}_{11}$. □

Together, Lemma 3.5 and Corollary 3.4 prove the main Theorem 3.6.

THEOREM 3.6. *The nodal functions of Loop subdivision, $\nu_i, i = 1 \dots N+6$, are linearly independent over $\mathbf{\Omega}$.*

The theorem sharply characterizes the locality of linear independence. On any finite union of $\mathbf{\Omega}_\ell$ the nodal functions are linearly dependent for sufficiently high valence. Only once we take the union to the limit $\mathbf{\Omega}$, do we obtain linear independence of the nodal functions for all possible valences.

Lemma 3.3 and Lemma 3.5 imply the analogous result for eigenfunctions.

COROLLARY 3.7. *For all N, the* eigenfunctions *φ_i, $i = 1, \dots N+6$, of Loop subdivision are linearly independent and form a basis for the Loop subdivision functions over $\mathbf{\Omega}$.*

In particular, we can now call the Loop eigenfunctions an *eigenbasis*.

4. Catmull Clark Subdivision. In this section, we investigate another widely used subdivision scheme, Catmull-Clark subdivision. The Catmull-Clark algorithm [3] accepts input meshes that have m-sided facets and vertices with N neighbors. However, all m-sided facets are split into m quadrilaterals in the first step as follows. A new face node is computed as the average of the facet vertices; a new edge node as the average of the edge endpoints and the two new face nodes of the faces joined by the edge; and a new vertex node of valence N is computed as

$$(Q + 2R + (N-3)S)/N$$

where Q is the average of the new face nodes of all faces adjacent to the old vertex, R is the average of the midpoints of all old edges incident on the old vertex point, and S is the old vertex point. A new quadrilateral facet then consists of consecutive edge node, vertex node, edge node and the face node. The rules are consistent with the Catmull-Clark stencils for quadrilateral meshes listed in Figure 4.1. The standard Catmull-Clark choices for α, β and γ are

$$\alpha := 1 - \frac{7}{4N}, \quad \beta := \frac{3}{2N^2}, \quad \gamma := \frac{1}{4N^2}.$$

If each node of a quadrilateral mesh facet has valence $N = 4$, Catmull-Clark subdivision amounts to tensor product bi-cubic spline subdivision. In this case, the

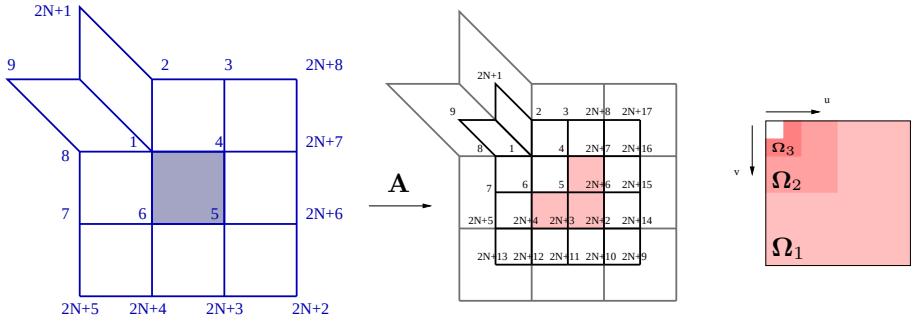

FIG. 4.2. *(left) Indices of Catmull-Clark nodes near a facet with one extraordinary node($N = 5$). (middle) The indices of the new control points after one subdivision. Three quarters of the domain now have well-defined tensor product B–spline structure. (right) The complete rectangular domain is composed of an infinite number of L shaped regions $\mathbf{\Omega}_\ell$.*

nodal functions are the standard tensor product uniform B–spline basis functions whose independence is well-documented. Since the extraordinary nodes (with valence $N \neq 4$) are always isolated after two subdivision steps, i.e. any two extraordinary nodes are separated by at least one node of valence four, we can focus our local analysis on surface parts adjacent to a single extraordinary node. That is, the subscript 0 refers to a mesh with isolated extraordinary nodes.

The indices of the $K := 2N + 8$ adjacent control points are stored in $\mathbf{c}_0$ as in Figure 4.2, *left*:

$$\mathbf{c}_0 := (\mathbf{c}_{0,1}, \dots \mathbf{c}_{0,K}).$$

After subdivision, the new set of $M := K + 9$ control vertices is ordered as shown in Figure 4.2, *middle* and stored in the vector:

$$\mathbf{c}_1 := (\mathbf{c}_{1,1}, \dots, \mathbf{c}_{1,K}, \mathbf{c}_{1,K+1}, \dots \mathbf{c}_{1,M}).$$

The subdivision rules are again denoted by

$$\mathbf{c}_1 = \mathbf{A}\mathbf{c}_0 \text{ where } \mathbf{A} := \begin{pmatrix} \mathbf{A}_{11} & 0 \\ \mathbf{A}_{21} & \mathbf{A}_{22} \\ \mathbf{A}_{31} & \mathbf{A}_{32} \end{pmatrix}.$$

Here $\mathbf{A}_{11}$ is an $(2N + 1) \times (2N + 1)$ matrix that computes the new extraordinary node and the vertices adjacent to it; $\mathbf{A}_{21}$ and $\mathbf{A}_{22}$ determine the seven vertices with indices $2N + 2, \dots, 2N + 8$, in the middle vertex ring; and $\mathbf{A}_{31}$ and $\mathbf{A}_{32}$ compute the last nine vertices with indices $2N + 9, \dots, 2N + 17$. We have enough control points in $\mathbf{c}_1$ to evaluate three regular patches (see shaded area in Figure 4.2, *middle*). The first K control points of $\mathbf{c}_1$,

$$(\mathbf{c}_{1,1}, \mathbf{c}_{1,2}, \dots, \mathbf{c}_{1,K}) = \mathbf{A}^\circ \mathbf{c}_0 := \begin{pmatrix} \mathbf{A}_{11} & 0 \\ \mathbf{A}_{21} & \mathbf{A}_{22} \end{pmatrix} \mathbf{c}_0,$$

are used as the control points for the next subdivision step. $\mathbf{A}^\circ$ can always be diagonalized by its eigenvectors $\mathbf{V}$:

$$\mathbf{A}^\circ = \mathbf{V}\mathbf{\Lambda}\mathbf{V}^{-1}.$$

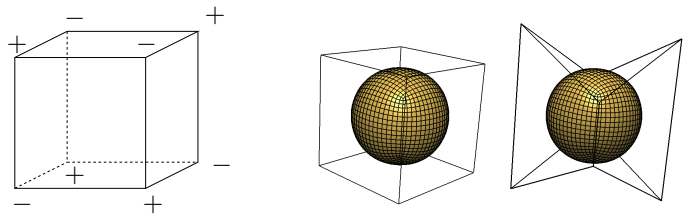

FIG. 4.3. *Global linear dependence of Catmull-Clark subdivision. ((left)) An alternative representation of the zero function with + indication any nonzero number and − its negative value. (right) Two control nets with the connectivity of a cube but different node positions. They generate the same Catmull-Clark surface!*

All eigenvalues are nonzero, except for $N = 3$ when one eigenvalue is zero. (The second eigenvalue of the zero Fourier block.) For $N > 3$, the linear independence of the nodal functions on $\mathcal{A}$ follows, just as in the case of Loop subdivision, from the local linear independence of tensor-product splines and the full rank of $\mathbf{A}^\circ$. The full rank of $\mathbf{A}_{11}$ implies *global linear independence* for $N > 3$.

The case $N = 3$ merits closer scrutiny.

LEMMA 4.1. *The nodal functions of Catmull-Clark subdivision corresponding to the graph in Figure 4.3 are (globally) linearly dependent.*

Proof. Given the displayed choice of nonzero values at the vertices, all new face nodes have value 0 and all averages of two old nodes connected by an edge have value 0. Therefore all new edge nodes have value zero and so do the new vertex nodes: $(Q + 2R + (N - 3)S)/N = (0 + 0 + 0S)/3 = 0$. □

Figure 4.3, *right*, illustrates dependence as the nonuniqueness of the control net for a given surface. Interestingly, an early version of the Catmull-Clark subdivision algorithm, quoted by Doo and Sabin [6], can be shown to be locally linearly independent for $N = 3$. Here a new vertex node of valence N is computed as $(Q + R + 2S)/4$.

In general, on $\cup_{i=2}^{\infty}\mathbf{\Omega}_i$, the nodal functions associated with the mesh for $N = 3$ are locally linearly dependent as illustrated in Figure 4.4. On $\mathbf{\Omega}_1$, if at least one node involved has valence $N \neq 3$ then $\mathbf{A}$ has full rank and the nodal functions are linearly independent. This implies global linear independence.

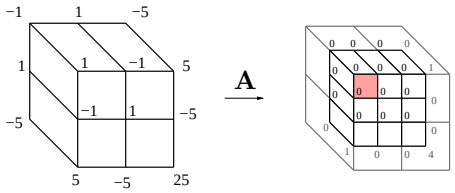

FIG. 4.4. *Nonzero input coefficients of the eigenfunction corresponding to the eigenvalue zero generating the zero function on $\cup_{i=2}^{\infty}\mathbf{\Omega}_i$ (shaded area).*

Therefore we have:

LEMMA 4.2. *The nodal functions of Catmull-Clark subdivision with support on $\mathcal{A}$ are linearly independent over $\mathcal{A}$ unless their nodes all have valence $N = 3$.*

5. Local linear independence of Catmull-Clark subdivision. Since the valence N can be arbitrary but each layer of the subdivision function corresponding to a region $\mathbf{\Omega}_\ell$ is defined by a finite number of B-spline control points, the nodal functions

of Catmull-Clark subdivision can not in general be locally linearly independent over any subset of $\mathbf{\Omega}$.

LEMMA 5.1. *The nodal functions of Catmull-Clark subdivision are locally linearly independent if and only if* $N = 4$.

Proof. For $N = 3$, the nodal functions are not linearly independent over $\cup_{i=2}^{\infty}\mathbf{\Omega}_i$ due to the example given in Figure 4.4.

If $N = 4$, the local linearly independence follows from the local linearly independence of tensor product B–splines.

For $N = 5$, the nodal functions are independent on $\mathbf{\Omega}_1$, (which implies linear independence on $\cup_{\ell=1}^{k}\mathbf{\Omega}_\ell$ since all eigenvalues are positive) and on any subset of $\mathbf{\Omega}_1$ that straddles at least two of the three quad subdomains of $\mathbf{\Omega}_1$ on which the subdivision surface is a single polynomial. However, due to the dimension of a polynomial piece (16), on any single one of the subdomains, the $2N + 8$ nodal functions must be linearly dependent.

For $N > 5$, the nodal functions are linearly dependent on $\mathbf{\Omega}_1$. □

Just as for Loop subdivision, for any k there exists a valence N so that the nodal functions ν_i of Catmull-Clark subdivision with support on $\mathbf{\Omega}_k$ are locally linearly dependent on $\mathbf{\Omega}_k$ and even on $\cup_{\ell=1}^{k}\mathbf{\Omega}_\ell$. The pattern, verified by symbolic calculation for isolated extraordinary nodes up to $N = 20$, is as follows.

CONJECTURE 2. *For* $k := N - 4 > 0$*, the nodal functions of Catmull-Clark subdivision* $\nu_i, i = 1 \dots 2N+8$ *are linearly independent on* $\cup_{i=1}^{k}\mathbf{\Omega}_i$ *but linearly dependent on* $\cup_{i=1}^{k-1}\mathbf{\Omega}_i$.

Next, we show that this characterization of the localness of linear independence is sharp: once we take the union of regions to the limit $\mathbf{\Omega}$, the nodal functions are linearly independent regardless of valence. As before, we first prove independence over $\mathbf{\Omega}$ of the eigenfunctions defined by the column vectors in $\mathbf{V}$. Then we conclude independence of the nodal functions for Catmull-Clark subdivision over $\mathbf{\Omega}$. As always, to be scalable, the control net of an eigenfunction is only well-defined if the extraordinary node is isolated.

LEMMA 5.2. *The eigenfunctions of Catmull-Clark subdivision are linearly independent over* $\mathbf{\Omega}$.

Proof. For $N > 3$, analogous to the proof of Lemma 3.3, we can reduce the problem to the independence of the eigenfunctions associated with the same eigenvalue.

According to [1, 2, 9], the eigenvalues of $\mathbf{A}_{11}$,

$$\lambda_k := \frac{1}{16}(C_k + 5 \pm \sqrt{(C_k + 9)(C_k + 1)}), \quad k = 1, \dots N - 1,$$

each have multiplicity two. We have $\lambda_k \neq 0$ since $(C_k+5)^2 \neq (C_k+9)(C_k+1)$. When $k \neq N/2$, the associated eigenvectors $\mathbf{u}_k$ and $\mathbf{w}_k$ are (see [16]):

$$\mathbf{u}_k = \begin{pmatrix} 0 \\ 4\lambda_k - 1 \\ 1 + C_k \\ (4\lambda_k - 1)C_k \\ C_k + C_{2k} \\ \vdots \\ (4\lambda_k - 1)C_{(N-1)k} \\ C_{(N-1)k} + 1 \end{pmatrix} \quad \text{and} \quad \mathbf{w}_k = \begin{pmatrix} 0 \\ 0 \\ S_k \\ (4\lambda_k - 1)S_k \\ S_k + S_{2k} \\ \vdots \\ (4\lambda_k - 1)S_{(N-1)k} \\ S_{(N-1)k} \end{pmatrix},$$

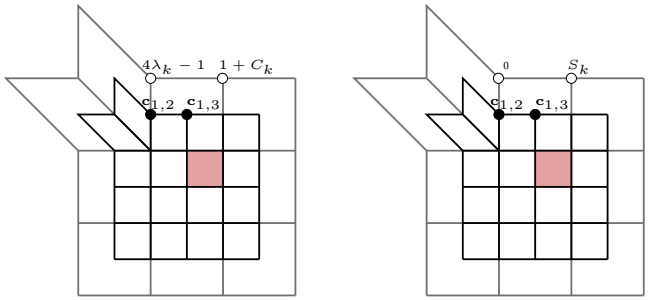

FIG. 5.1. *The B-spline control points* $\mathbf{c}_{1,2}, \mathbf{c}_{1,3}$ *(red points) used to certify that the eigenfunctions associated with* $\mathbf{u}_k$ *and* $\mathbf{w}_k$ *are independent.*

where $C_k := \cos(2\pi k/N)$ and $S_k := \sin(2\pi k/N)$. To show that the two eigenfunctions defined by $\mathbf{u}_k$ and $\mathbf{w}_k$ are linearly independent, we consider the tensor-product B–spline entries $\mathbf{c}_{1,2}$ and $\mathbf{c}_{1,3}$ of $\mathbf{c}_1|_{\mathbf{c}_0=\mathbf{u}_k}$ and $\mathbf{c}_1|_{\mathbf{c}_0=\mathbf{w}_k}$ (solid dots in Figure 5.1). The two eigenfunctions are linearly independent over the shaded region if they generate independent B–spline control points $\mathbf{c}_{1,2}$ and $\mathbf{c}_{1,3}$, i.e. if

$$\det \begin{pmatrix} \mathbf{c}_{1,2}|_{\mathbf{c}_0=\mathbf{u}_k} & \mathbf{c}_{1,3}|_{\mathbf{c}_0=\mathbf{u}_k} \\ \mathbf{c}_{1,2}|_{\mathbf{c}_0=\mathbf{w}_k} & \mathbf{c}_{1,3}|_{\mathbf{c}_0=\mathbf{w}_k} \end{pmatrix} = \lambda_k^2 \det \begin{pmatrix} 4\lambda_k - 1 & 1 + C_k \\ 0 & S_k \end{pmatrix} \neq 0.$$

In fact,

$$\begin{aligned} & 4\lambda_k - 1 \neq 0 \\ \iff & \frac{1}{4}(C_k + 5 \pm \sqrt{(C_k + 9)(C_k + 1)}) \neq 1 \\ \iff & (C_k + 5) \pm \sqrt{(C_k + 9)(C_k + 1)}) \neq 4 \\ \iff & (\pm\sqrt{(C_k + 9)(C_k + 1)}) \neq -1 - C_k \\ \iff & (C_k + 9)(C_k + 1) \neq (-1 - C_k)^2 \\ \iff & 8C_k + 8 \neq 0 \\ \iff & C_k \neq -1. \end{aligned}$$

$C_k \neq -1$ and $S_k \neq 0$ follows from $k \neq N/2$.

When $k = N/2$, the eigenvectors of $\lambda_k = \frac{1}{4}$ are

$$\begin{aligned} \mathbf{u}_k^T &= (0, 1, 0, -1, 0, 1, 0, \ldots, -1, 0, \ldots) \quad \text{and} \\ \mathbf{w}_k^T &= (0, 0, 1, 0, -1, 0, 1, \ldots, 0, -1, \ldots) \end{aligned}$$

then

$$\det \begin{pmatrix} \mathbf{c}_{1,2}|_{\mathbf{c}_0=\mathbf{u}_k} & \mathbf{c}_{1,3}|_{\mathbf{c}_0=\mathbf{u}_k} \\ \mathbf{c}_{1,2}|_{\mathbf{c}_0=\mathbf{w}_k} & \mathbf{c}_{1,3}|_{\mathbf{c}_0=\mathbf{w}_k} \end{pmatrix} = \lambda_k^2 \det \begin{pmatrix} 1 & 0 \\ 0 & 1 \end{pmatrix} \neq 0.$$

For the eigenvalues of $\mathbf{A}_{22}$, $\{\frac{1}{8}, \frac{1}{8}, \frac{1}{16}, \frac{1}{16}, \frac{1}{32}, \frac{1}{32}, \frac{1}{64}\}$, the eigenfunctions are the tensor-product power basis functions ([16])

$$\{u^3, v^3, u^3 v, u v^3, u^3 v^2, u^2 v^3, u^3 v^3\}$$

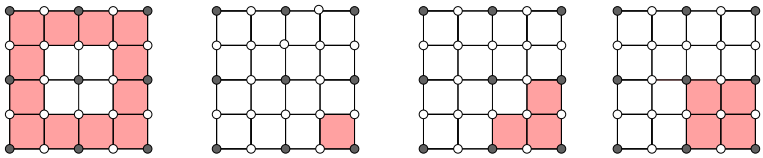

FIG. 5.2. *Summary of findings for Catmull-Clark subdivision. Domains G (shaded) and valence N for which the nodal functions with support on G are linearly independent.*

whose pairwise independence is well known.

For the special case $N = 3$, there is a zero eigenvalue and, as illustrated in Figure 4.4, the associated eigenfunction has zero values on $\cup_{i=2}^{\infty}\mathbf{\Omega}_i$. But the remaining eigenfunctions are linearly independent on $\cup_{i=2}^{\infty}\mathbf{\Omega}_i$ and, if at least one neighbor of the central node has valence $N \neq 3$, the zero eigenfunction has non-zero values on $\mathbf{\Omega}_1$. □

Since the transformation between the eigenfunctions and nodal functions are invertible, provided the extraordinary node is surrounded by regular nodes, all such nodal functions are linearly independent and form a basis when the eigenfunctions do. If the nodal functions were the result of one refinement, full rank of $\mathbf{A}_{11}$ (unless all relevant nodes have valence $N = 3$) establishes the main result.

THEOREM 5.3. *The nodal functions of Catmull-Clark subdivision that have support on $\mathbf{\Omega}$ are linearly independent over $\mathbf{\Omega}$ unless their nodes all have valence $N = 3$.*

6. Primal schemes. We now collect the key ideas of the preceeding analyses. An extraordinary node is a control net node of valence different from the 'regular' majority. A subdivision scheme is called primal if there exists a sequence of extraordinary nodes converging towards each extraordinary point. While the typical application of subdivision creates a parametrized surface in $\mathbb{R}^3$, for the analysis, it is sufficient to look at one spatial coordinate since the coordinates do not interact.

Subdivision surfaces can be understood as generating surfaces as a union of surface rings that converge towards extraordinary points [14]. Let $\mathcal{A} := \{1, \ldots, N\} \times \mathbf{\Omega}_1$ be the domain of the first surface ring. An extraordinary node of a primal scheme is called isolated if at least one surface ring separates it from any other extraordinary node. That is, $\mathcal{A}$ is well-defined if the extraordinary node is isolated. Let $\{g_i\}$ be the nodal functions, corresponding to a regular subnet and typically box-splines, that generate the first subdivision surface ring. Denote by A_* the refinement matrix from the input control net to a control net with isolated extraordinary node. This may be the identity if all extraordinary nodes are already isolated. To show that the nodal functions of a subdivision scheme are (globally) linearly independent, we focus on $\mathcal{A}$.

LEMMA 6.1 (global linear independence). *If the functions g_i are linearly independent and the matrix A_* is of full rank then the nodal functions ν_j of the subdivision are globally linearly independent.*

Proof. By assumption, the nodal functions g_i of the once-refined control net are linear independent on the union of all local domain rings $\mathcal{A}$. Since A_* is of full rank and, as a refinement matrix, its rank is less than the number of g_i, the coefficients of the input control net are zero. □

For example, if the functions g_i are four-direction box splines, then the nodal functions are not globally independent since this space of splines has dependent gen-

erating g_i [5]. The example of Figure 4.3 underscores the need for the assumption on A_*. – A counting argument shows that typical schemes are not locally linearly independent.

LEMMA 6.2 (local dependence for high valences). *Let ν_0 be the nodal function associated with an extraordinary node of valence N and ν_ℓ, $\ell = 1, \dots, N$ the nodal functions of its direct neighbor nodes. Denote by x_i^m the ith segment of the mth surface ring and assume that x_i^m belongs to a space of fixed finite dimension that is independent of N. If each ν_j has support on $\mathbf{\Omega}_k$ for all $k \geq k_0$ then there exists $m \in \mathbb{Z}$ so that ν_ℓ, $\ell = 0, \dots, n$ are* locally linearly dependent *on $\mathbf{\Omega}_m$.*

Proof. For sufficiently large valence N, the number of ν_j with support on the domain of x_i^m exceeds the fixed dimension of the space from which x_i^m is drawn. □

The assumptions of the Lemma hold in particular for symmetric C^1 subdivision schemes derived from box-splines since each x_i^m is finitely generated and the ν_j must all interact at the extraordinary point to guarantee smoothness and partition of unity. For such schemes, nodal functions contribute to the whole spline ring x^m of high valence only after a number of subdivision steps k_0.

As the example in Figure 4.4 shows, failure of the counting argument for low valences does not imply that the nodal functions are locally linearly independent. To establish local linear independence and also to find the m in Lemma 6.2 beyond which the nodal functions are locally linearly dependent, requires an analysis specific to each scheme.

To investigate linear independence on the domains $\mathbf{\Omega}$, corresponding to control facets surrounding an extraordinary node, we use eigenfunctions.

LEMMA 6.3 (linear independence of eigenfunctions). *The eigenfunctions φ_i, $i = 1, \dots, k$ are linearly independent on $\mathbf{\Omega}$ if the eigenfunctions corresponding to each eigenvalue, sepearately, are independent.*

Proof. Let λ_i be sorted by absolute value and $\lambda_0 = 1$. Suppose there exist scalars $a_1, a_2, \dots a_k$, not all zero, such that $\sum_{i=1}^k a_i \varphi_i = 0$. Let λ_j be an absolute largest eigenvalue such that $a_j \neq 0$. If $\lambda_j = 0$ then the eigenfunctions to the eigenvalue 0 are dependent contradiciting the assumptions. If $\lambda_j \neq 0$ then, with $w_i := -a_i/a_j$, we can write $\varphi_j = \sum_{i=j+1}^k w_i \varphi_i$. and, by the defining property of eigenfunctions, for any $(u, v) \in \mathcal{A}$,

$$\varphi_j(\frac{u}{2^m}, \frac{v}{2^m}) = \sum_{i=j+1}^{k} w_i \varphi_i(\frac{u}{2^m}, \frac{v}{2^m}) \quad \Rightarrow \quad \varphi_j(u, v) = \sum_{i=j+1}^{k} w_i (\frac{\lambda_i}{\lambda_j})^m \varphi_i(u, v).$$

Since the equality has to hold for all m and $(\frac{\lambda_i}{\lambda_j})^m$ goes to zero or repeatedly changes sign, this implies $\varphi_j = \sum_{i:\lambda_i = \lambda_j} w_i \varphi_i$. That is the eigenfunctions associated with the same eigenvalue λ_j must be linearly dependent in contradiction to the assumption. □

While the, possibly generalized, eigenvectors of an eigenvalue are independent, checking that the corresponding eigenfunctions are independent requires an analysis specific to each scheme.

We can now characterize when the nodal functions ν_i are linearly independent.

COROLLARY 6.4. *If the refinement matrix A_* from the input mesh to a mesh with isolated extraordinary nodes is of full rank and, for each eigenvalue, the corresponding eigenfunctions are independent then the nodal functions $\nu_i, i = 1 \dots K$ are linearly independent on $\mathbf{\Omega}$.*

Proof. If the extraordinary node is isolated then nodal functions and eigenfunctions are related by the invertible matrix V of the generalized eigenvectors of the

Jordan decomposition of the subdivision matrix:

$$[\varphi_1, \ldots, \varphi_k] = V[\nu_1, \ldots, \nu_k].$$

The general case follows by subdivision and the full rank of A_*. □

Corollary 6.4 and Lemma 6.2 characterize the locality of linear independence of subdivision schemes. On any finite union of $\mathbf{\Omega}_\ell$ the nodal functions are linearly dependent for sufficiently high valence. On the infinite union $\mathbf{\Omega}$, the nodal functions are typically linear independent provided the underlying regular spline functions g_i are. Subtle exceptions, illustrated by the examples in Figures 4.3 and 4.4, underscore the need for the assumption on A_*.

7. Summary and related open issues. The characterization of linear independence is a vital part of the foundations of generalized subdivision and illuminates the numerical properties of the nodal functions. It imparts a cautionary note for computational use: near vertices of high valence, the nodal functions may not be linearly independent.

Closely related to independence is the characterization of the *condition number* of subdivision schemes. Analoguous to the condition of splines, the condition of subdivision schemes adresses the question how small the limit surface can be when the input mesh has unit diameter: the condition number is inverse proportional to the diameter of the surface. Control net designers have been grappling with this issue, for example when forced to grossly exagerate tetrahedral features while modeling with Loop subdivision. Indeed, the example of Figure 4.3 shows that the condition number of Catmull-Clark subdivision nodal functions can be infinite. Based on these examples, one can guess that low valences, in particular $N = 3$, yield large condition numbers. But clearly, the condition of subdivision merits further attention.

Acknowledgements: This work was supported in part by NSF grants DMI-0400214. and CCF-0430891.

REFERENCES

[1] A. A. Ball and D. J. T. Storry, *Conditions for tangent plane continuity over recursively generated B-spline surfaces*, ACM Trans. on Graphics, 7 (1988), pp. 83–102.
[2] A. A. Ball and D. J. T. Storry, *An investigation of curvature variations over recursively generated B-spline surfaces*, ACM Transactions on Graphics, 9 (1990), pp. 424–437.
[3] E. Catmull and J. Clark, *Recursively generated B-spline surfaces on arbitrary topological meshes*, Computer Aided Design, 10 (1978), pp. 350–355.
[4] Fehmi Cirak, Michael Ortiz, and Peter Schröder, *Subdivision surfaces: A new paradigm for thin-shell finite-element analysis*, Internat. J. Numer. Methods Engineering, 47 (2000), pp. 2039–2072. page 2050.
[5] C. de Boor, K. Höllig, and S. Riemenschneider, *Box splines*, vol. 98 of Applied Mathematical Sciences, Springer-Verlag, New York, 1993.
[6] D. Doo and M. Sabin, *Behaviour of recursive division surfaces near extraordinary points*, Computer-Aided Design, 10 (1978), pp. 356–360.
[7] Eitan Grinspun, *The Basis Refinement Method*, PhD thesis, California Institute of Technology, May 16 2003. page 39.
[8] Eitan Grinspun, Petr Krysl, and Peter Schröder, *CHARMS: A simple framework for adaptive simulation*, in SIGGRAPH 2002 Conference Proceedings, John Hughes, ed., Annual Conference Series, ACM Press/ACM SIGGRAPH, 2002, pp. 281–290.
[9] K. Karciauskas, J. Peters, and U. Reif, *Shape characterization of subdivision surfaces – case studies*, 21 (2004), pp. 601–614.
[10] Charles T. Loop, *Smooth subdivision surfaces based on triangles*, 1987. Master's Thesis, Department of Mathematics, University of Utah.

[11] Michael Lounsbery, Tony D. DeRose, and Joe Warren, *Multiresolution analysis for surfaces of arbitrary topological type*, ACM Transactions on Graphics, 16 (1997), pp. 34–73. page 18.

[12] A. H. Nasri, *Polyhedral subdivision methods on free-form surfaces*, ACM Transactions on Graphics, 6 (1987), pp. 29–73.

[13] J. Peters and U. Reif, *Shape characterization of subdivision surfaces – basic principles*, Computer Aided Geometric Design, 21 (2004), pp. 585–599.

[14] Ulrich Reif, *A unified approach to subdivision algorithms near extraordinary vertices*, Computer Aided Geometric Design, 12 (1995), pp. 153–174. ISSN 0167-8396.

[15] Jos Stam, *Evaluation of Loop subdivision surfaces*, 1998. SIGGRAPH 98 Proceedings notes.

[16] ———, *Exact evaluation of Catmull-Clark subdivision surfaces at arbitrary parameter values*, in SIGGRAPH 98 Proceedings, Michael Cohen, ed., Addison Wesley, 1998, pp. 395–404.

[17] Luiz Velho and Denis Zorin, *4-8 subdivision*, Computer Aided Geometric Design, 18 (2001), pp. 397–427.

[18] D. Zorin. Smoothness of stationary subdivision on irregular meshes. *Constr. Approx.*, 16(3):359–397, 2000.